JOURNAL OF GEOPHYSICAL RESEARCH, VOL. 95, NO. A8, PAGES 11,957–11,965, AUGUST 1, 1990

Magnetic Field Structure of Interplanetary Magnetic Clouds at 1 AU

R. P. LEPPING

Laboratory for Extraterrestrial Physics, NASA Goddard Space Flight Center, Greenbelt, Maryland

J. A. JONES

ST Systems Corporation, Lanham, Maryland

L. F. BURLAGA

Laboratory for Extraterrestrial Physics, NASA Goddard Space Flight Center, Greenbelt, Maryland

Interplanetary magnetic clouds, although not dominant, are a relatively common feature of the solar wind at 1 AU. Their diameters at 1 AU fall in the range of 0.2–0.4 AU, and they have enhanced field strength ($B \simeq 15$–30 nT at 1 AU), and lower plasma temperature and density than the surrounding plasma. The internal field is a magnetic force-free configuration, and therefore the current density (J) is proportional to B everywhere: $J = \alpha B$, giving $\nabla \times B = \alpha B$. If α is constant throughout the cloud (Burlaga, 1988), then $\nabla^2 B = -\alpha^2 B$, which has a cylindrically symmetric field solution that is consistent with observations: the axial field is proportional to the zeroth-order Bessel function of r, where r is the perpendicular distance from the cloud's axis, the tangential component is proportional to the first-order Bessel function, and the radial component is zero. We have developed a least squares program that fits magnetic field data within a cloud to these functions and which estimates various properties of the cloud, such as its size, maximum B, and inclination of its axis, as well as closest approach distance of the spacecraft. Results of a study of 18 clouds observed at 1 AU indicate that the most probable direction of the cloud's axis is within 15° of the ecliptic plane and ≃100° from the Sun's direction when it is projected into the ecliptic plane. A broad range of orientations is observed with some extending to 80° from the ecliptic. Other statistical properties are presented, and three cases are discussed in detail.

INTRODUCTION

Interplanetary magnetic clouds are mesoscale (diameter: 0.2–0.4 AU at 1 AU) plasma and magnetic field structures having a large rotation in the field's direction, enhanced field strength, low plasma temperature and density (compared to the ambient plasma), and a low plasma β [*Burlaga et al.*, 1981]. They usually possess an approximately symmetric field strength, being largest near the center of the observing interval. They pass the Earth's orbit in about one day as observed by spacecraft at 1 AU [*Burlaga et al.*, 1981]. The study of such structures is important not only because it contributes to the understanding of the solar wind at these scales but also because of what the structures may tell us specifically about the manner in which the Sun ejects material and magnetic field, i.e., the structures are probably manifestations of coronal mass ejections (CMEs) [*Burlaga and Behannon*, 1982; *Wilson and Hildner*, 1984; *Marubashi*, 1986; *Whang*, 1988] and disappearing filaments [*Wilson and Hildner*, 1986]. Furthermore, it is becoming evident that magnetic clouds are often a dramatic source of long-lasting, strong, interplanetary, negative B_z fields (in solar magnetospheric coordinates), which is an optimum condition for solar wind–magnetosphere interaction via field line merging [e.g., *Burlaga et al.*, 1981; *Wilson*, 1987; *Zhang and Burlaga*, 1988]. Also, we know that magnetic clouds are often drivers of interplanetary shock waves [*Burlaga et al.*, 1981; *Klein and Burlaga*, 1982; R. P. Lepping, F. M. Ipavich, and L. F. Burlaga, A flare-associated shock pair at 1 AU and related magnetic cloud, submitted to *Journal of Geophysical Research*, 1989]. Hence, like interplanetary shocks, magnetic clouds provide us with a link between ejected material, field, and energy on the Sun and significant magnetospheric activity via the solar wind. There is also evidence [*Burlaga et al.*, 1981; *Badruddin et al.*, 1985; *Zhang and Burlaga*, 1988] that the turbulent sheath between the upstream shock and the front boundary of a large field structure can affect the propagation of cosmic rays in the manner discussed by *Morrison* [1954]. An example of this is given by R. P. Lepping et al. (submitted manuscript, 1989), who show a correlation of a Forbush decrease with a cloud passage at 1 AU. The ordered field of the cloud itself plays a similar role, but it has a more modest effect on decreasing the cosmic ray intensity. Observations and models of magnetic clouds are reviewed by *Burlaga* [1989].

Because of the importance of magnetic clouds and these relationships, we decided to develop a scheme, which partially depends on the least squares technique, for fitting the interplanetary magnetic field data obtained within an observed cloud to a model that has proven to be successful for describing cloud field structure, at least to first order. The model, based on *Lundquist*'s [1950] constant-α force-free field solution, was introduced by *Burlaga* [1988] and employed by him in fitting many cases with trial-and-error solutions with generally good results. However, this method can be time-consuming and does not guarantee an optimum solution. Our technique does provide an optimum solution in a sense to be explained below.

Paper number 90JA00227.
0148-0227/90/90JA-00227$05.00

The outline of this paper is as follows: we discuss the Burlaga model and its assumptions, estimate the proper "starting" coordinate system, outline the least squares technique for fitting the model to the data, present a few cases in detail, provide statistical results of the study of 18 cases, and speculate on the large-scale geometry of magnetic fields in clouds based on this and another study [*Burlaga et al.*, 1990].

THE MODEL

We assume that to a good approximation the magnetic cloud is (magnetic) force-free, i.e., $J = \alpha B$, so that

$$\nabla \times B = J = \alpha B \tag{1}$$

This model, with variable α, was proposed by *Goldstein* [1983] and used by *Marubashi* [1986] to fit two magnetic clouds. *Burlaga* [1988] showed that one can consider α approximately constant in describing magnetic clouds to first order. For constant α, equation (1) gives

$$\nabla \times (\nabla \times B) = \alpha(\nabla \times B) = \alpha^2 B \tag{2}$$

or

$$\nabla^2 B = -\alpha^2 B \tag{3}$$

since $\nabla \cdot B = 0$. Solutions to equation (3) in cylindrical coordinates in terms of the zeroth- and first-order Bessel functions were given by *Lundquist* [1950]:

Axial component

$$B_A = B_0 J_0(\alpha R) \tag{4a}$$

Tangential component

$$B_T = B_0 H J_1(\alpha R) \tag{4b}$$

Radial component

$$B_R = 0 \tag{4c}$$

where $H = \pm 1$, the sign providing the handedness of the field helicity, and where B_0 (the "amplitude") is an estimate of the magnitude of the field at maximum strength (which we will see occurs at the "axis" of the cloud) and R is the radial distance from the axis. This is the solution which *Burlaga* [1988] used to fit magnetic cloud observations by trial and error. *Ivanov et al.* [1989] proposed using a constant-α toroidally symmetric solution, and they suggested that the extra parameter provided by that model gives somewhat better fits than the cylindrically symmetric model.

Notice that all three components of B depend on only one independent variable, R, provided that the seven parameters defining a magnetic cloud's characteristics, relative to a spacecraft, are determined. These parameters are as follows: (1) θ and (2) ϕ (the latitude and longitude of the cloud's axis, usually given with respect to the ecliptic plane), i.e., the orientation of the cloud, (3) Y_0, distance of the spacecraft from the cloud axis at closest approach point, (4) B_0, magnetic field strength on the axis of the cloud, (5) α^{-1} (related to the size of the cloud), (6) $H = \pm 1$, the sign of the helicity, and (7) t_0, the time at closest approach to the cloud's axis.

Our justification for assuming that magnetic clouds are approximately magnetic force-free with constant α is based on the success we have had in fitting this model mainly to magnetic field data at 1 AU from various IMP spacecraft and from ISEE 3, as we show below. The observed stability of magnetic clouds [*Burlaga and Behannon*, 1982] is consistent with the arguments that constant-α force-free fields are relatively stable configurations as discussed by *Woltjer* [1958], *Suess* [1988], *Taylor* [1986], and *Yang* [1989]. Using the constant-α model (which henceforth we will refer to as the "Lundquist (1950) solution"] and various choices for free parameters, we simulated magnetic clouds for the purpose of determining a means of obtaining useful "principal" axes, in order to guide us in a choice of a first-order coordinate frame. It became evident that a field variance analysis [e.g., *Sonnerup and Cahill*, 1967] of these simulated cloud data yields useful principal axes, provided that the field is first unit normalized at each point (below we justify this).

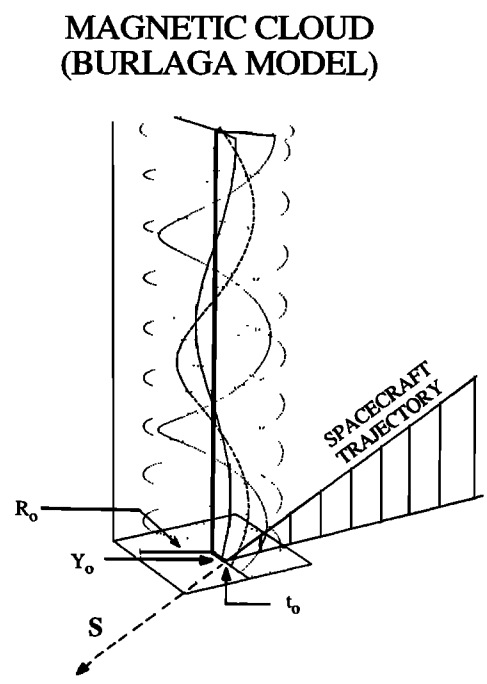

Fig. 1. A computer simulation of the field lines in a magnetic cloud based on the *Lundquist* [1950] solution, where R_0 is the radius of the cloud and S is a unit vector parallel to the trajectory of a spacecraft intersecting the cloud at closest-approach distance Y_0 and at time t_0.

Figure 1 shows the field lines within a computer-simulated magnetic cloud. Notice that the field is a straight line along the axis of the cloud (shown as a solid line where the field is maximum) and changes to helical lines as we move away from the axis, finally becoming circles at the boundary (shown at top and bottom). The figure shows the density of the curves decreasing as we go outward from the cloud's axis, representing decreasing field strength. That is, we first see a heavy solid straight line on the axis, then dashed spiral curves of moderate density and moderate pitch angle, and finally low-density dotted curves of large pitch near the boundary. Also shown in the figure is the spacecraft trajectory, denoted by the unit vector S. We call the cloud's axis the Z axis, and the cross product $Z \times S$ is the Y axis. Finally, as usual $Y \times Z = X$.

Field variance analyses of the simulated clouds reveal that the X, Y, and Z axes are "near" the minimum, maximum,

and intermediate variance directions, respectively. How near these axes are to the variance directions depends on how far away from the simulated cloud's axis the spacecraft passes. For example, the angle between true X and estimated X was seen to depend on the relative closest-approach distance, "RD" = $|Y_0|/R_0$ is the cloud's true radius, in the following way: for RD = 0.3 the angle is 3.1°, for RD = 0.6 the angle is 8.3°, and for RD = 0.9 the angle is 17.8°. Later it will be seen that our cloud data provide us with RDs no greater than ≈0.7, so that the difference in orientation between the true and estimated axes, based on the variance analyses, is always less than 11.0° and often much less. In any case, our estimation of a cloud's axes does not depend solely on the variance analysis, as we see below. We call the variance (orthogonal) coordinate system the estimated cloud system, where the axes are denoted by X_v, Y_v, Z_v. It is obvious that two of these three axes (X_v and Y_v) depend on the path the spacecraft takes through the cloud. (Since Z_v is an estimate of the cloud's axis, it is ideally independent of the spacecraft's trajectory, of course.) We show the cloud with its symmetry axis (Z) standing vertically in the figure, but clouds travel outward from the Sun with various attitudes (and with various closest-approach distances), as studies have shown [*Burlaga*, 1988], and as we will confirm. Therefore the angle between the vectors S and Z can be expected to occur with a distribution of values over 360°, and the closest-approach distance can be anything from 0 to R_0, the radius of the cloud. We should point out here that the sketch in Figure 2 of *Elphic and Russell* [1983], which is used to describe cylindrically symmetric flux ropes at Venus, is qualitatively similar to the field lines in our Figure 1. They also perform a variance analysis to determine principal axes. However, because we apply the technique to unit normalized field vectors, whereas they do not (and possibly also due to the specific nature of our two different models for representing the field lines which give different pitch angles), our eigenvectors Y_v and Z_v have reversed roles. It appears that X_v (which they call k) shares the same role in both models; it is the minimum variance direction.

Time domain plots of B, θ, and ϕ, in a cloud simulated according to the constant-α model versus actual B observations, showed various degrees of agreement. Field directions (θ, ϕ) often showed good to remarkable agreement, whereas the magnitudes (B) showed usually only qualitative agreement, i.e., actual data were skewed in B, but simulated B was symmetric according to the model. This is what guided us to start the analysis by unit normalizing the basic field vectors within the cloud, as mentioned above, in order to deliberately give greater weight to field direction over magnitude. (Also, this method of obtaining a first estimate of the cloud's principal axes was usually superior to the standard method.) Later we scaled the field in a one-parameter (B_0) least squares fit to the data; B_0 is the "amplitude" shown in equations (4).

The least squares fit of the data to the model in the variance coordinate system is a minimization of χ^2, where

$$\chi^2 = \sum [(B^O_{xv} - B^M_{xv})^2 + (B^O_{yv} - B^M_{yv})^2 + (B^O_{zv} - B^M_{zv})^2]/N \quad (5)$$

and where the subscript v refers to the variance coordinate system, superscripts M and O refer to the model and observed fields, respectively, and N is the number of field vectors (hour averages were used in this study). It is understood at this stage that $\mathbf{B}^M$ and $\mathbf{B}^O$ are unit normalized; therefore χ^2 is dimensionless. (In practice the direction S need not be known to estimate the cloud's axis; all that is necessary is that the variance axes be obtained. Also for convenience, B_0 is set equal to 1.) The least squares analysis provides estimates of the following quantities: (1) the origin (i.e., the point along the cloud's axis at closest approach); this is equivalent to finding the cloud's center time, t_0, (2) Y_0, (3) a correction to attitude of the axis: $\Delta\theta_1$ and $\Delta\phi_1$, (4) R_0 (= $2.4/\alpha$) (the factor 2.4 arises from the first zero of the $J_0(\alpha R)$ Bessel function, i.e., B_A is zero on the cloud's boundary), and (5) $H = \pm 1$. After these parameters are estimated, they are used in the model to refine the cloud's attitude (with the $\Delta\theta_1$ and $\Delta\phi_1$ adjustments), and then the least squares fit to the origin, Y_0, R_0, and H is repeated. Again $\Delta\theta$ and $\Delta\phi$ are obtained iteratively, now called $\Delta\theta_2$ and $\Delta\phi_2$, but these are not again used to refine the fit. Instead, they are combined into a single angle δ, which is that angle between the axis of the cloud for the final solution and the next iteration (which is not obtained). The angle δ is considered a means of judging the quality of the fit along with the value of χ^2 (final) and the symmetry of B^M, which will be discussed below. That is, large values of δ indicate that convergence probably is not being achieved. The last determination of the cloud's axis is represented by θ_0, ϕ_0 with respect to the ecliptic plane where $\phi_0 = 0°$ is sunward. Finally, a single least squares fit to B_0 (the maximum field on the axis of the cloud) is made, as mentioned above. We now discuss the application of this scheme to magnetic field data obtained by spacecraft.

OBSERVATIONS

Interplanetary magnetic field and plasma data taken at 1 AU over many years by ISEE 3 and various IMP spacecraft were examined in the form of hourly averages to obtain examples of magnetic clouds. This study is primarily based on the list of 19 events identified by *Zhang and Burlaga* [1988]. All of these events were analyzed, but seven did not meet our criteria for a good fit. We also analyzed six additional (and acceptable) events that were discussed in recent papers, i.e., events on day 364 of 1967 and day 174, 1971 [*Burlaga*, 1988]; day 42, 1969, and day 321, 1975 [*Klein and Burlaga*, 1982]; day 306, 1972 [*Ipavich and Lepping*, 1975]; and day 327, 1982 [*Burlaga et al.*, 1987]. Hence a total of 18 "acceptable" clouds were used in the remainder of the study. The criteria used for the discrimination were the size (~1 day) and physical characteristics listed in the introduction, namely, enhanced B over background values, low β, symmetrical structure as seen in θ and ϕ (i.e., as seen in the rotation of the magnetic field), and low B-rms/B. Table 1 gives the dates, start/end times, and associated spacecraft for the 18 clouds; other quantities in the table will be discussed below. We will discuss in some detail three of these clouds, one being typical and the others being extreme cases with regard to the tilt of their axes. The "typical" one lies approximately in the ecliptic plane ($\theta_0 = 10°$). We will discuss it first.

Figure 2 shows combined IMP 8 and ISEE 3 magnetic field data around a magnetic cloud occurring on days 354 and 355 of 1980. The cloud's assumed start and end times are marked by vertical lines on the figure; these times are listed in Table 1. It is a matter of subjective judgment just where to put these endpoints. Some trial and error was involved in their

TABLE 1. Magnetic Clouds at 1 AU: Estimated Characteristics

		Start[b]		End[c]																Spacecraft[r]	
No.[a]	Year	Day	Hour	Day	Hour	ΔT[d]	t_0[e]	ϕ_0[f]	θ_0[g]	R_0[h]	Y_0[i]	B_0[j]	H[k]	$\lvert Y_0\rvert/R_0$	χ^2[l]	δ[m]	SF[n]	V_c[o]	V_b[p]	ΔV[q]	MAG	Plasma
1	67	364	10	365	22	34	17.2	96°	−45°	29.8	1.1	15.8	+	0.04	0.98	0.0°	0.56	429	473	40	I1	I2
2	69	42	9	43	17	32	20.0	252°	−29°	27.3	13.8	16.0	+	0.51	1.26	14.2°	0.70	442	531	90	H, I2	I1
3	71	174	9	175	6	21	11.1	85°	58°	11.6	−1.5	12.1	−	0.13	0.52	0.1°	0.59	341	345	4	I5, I6	I6 (LANL)
4	72	306	2	306	20	18	4.9	107°	−2°	19.1	−4.3	30.1	−	0.23	1.01	7.5°	0.35	490	664	170	I7	Merge (LANL)
5	75	321	2	322	5	27	12.1	168°	−80°	14.9	10.9	20.5	−	0.73	2.02	0.5°	0.51	367	398	30	I8	I8
6	78	4	17	5	20	27	9.2	350°	34°	35.3	18.2	21.9	+	0.52	1.88	3.6°	0.41	549	660	110	I8	I8
7	78	93	18	94	8	14	5.0	290°	33°	15.6	0.7	13.7	+	0.05	2.45	4.1°	0.44	473	490	20	I8	I8
8	78	156	8	157	14	30	17.1	219°	−61°	23.4	13.8	12.9	−	0.59	4.55	11.1°	0.62	481	553	70	I8	I8 (LANL)
9	78	239	19	240	16	21	11.0	44°	−72°	15.0	−0.5	22.8	−	0.03	2.89	0.7°	0.54	460	406	−50	I3, I8	I8 (LANL)
10	78	302	23	304	0	25	14.8	116°	−64°	16.3	−0.4	14.0	−	0.03	0.65	0.0°	0.65	392	423	30	I3, I8	I8, I3
11	79	261	15	262	18	27	10.8	132°	78°	20.8	9.7	15.8	−	0.47	1.17	6.1°	0.44	367	400	30	I3	I3
12	80	47	1	48	6	29	14.4	76°	−30°	21.7	−0.8	17.8	−	0.04	0.67	0.2°	0.55	378	427	50	I3	I3
13	80	79	18	81	11	41	17.1	102°	4°	22.1	−3.5	17.4	+	0.16	0.90	1.4°	0.47	326	377	50	I3, I8	I3, I8
14	80	354	12	355	14	26	14.0	105°	10°	19.8	−1.4	36.1	−	0.07	0.43	0.0°	0.59	504	478	−30	I3, I8	I3, I8
15	81	38	7	39	12	29	16.5	172°	12°	38.5	−5.6	12.9	−	0.15	0.84	3.6°	0.63	446	496	50	I3, I8	I3, I8
16	81	64	13	65	7	18	14.0	314°	−72°	19.5	3.0	20.2	+	0.15	0.96	4.2°	0.85	553	588	40	I3, I8	I3, I8
17	82	268	17	269	15	22	14.3	111°	10°	16.4	−2.1	24.8	+	0.13	3.20	0.7°	0.68	482	404	−80	I8	I3, I8
18	82	327	21	328	12	15	4.8	254°	−56	16.1	0.7	28.1	+	0.04	2.33	2.3°	0.31	547	495	−50	I8, I3	I8

[a]The code number of the cloud.
[b]The day of year and the hour of day (UT) at the beginning of the magnetic cloud interval.
[c]The day and hour (UT) at the end of the cloud interval, inclusive.
[d]The duration of the cloud interval in hours.
[e]The time from the start to the closest approach to the cloud's axis, in hours.
[f]The longitude of the cloud's axis measured counterclockwise in an ecliptic coordinate system, where $\phi_0 = 0°$ represents toward the Sun.
[g]The latitude of the cloud's axis in an ecliptic coordinate system.
[h]The estimated radius of the cloud in units of 10^6 km.
[i]The closest approach distance in units of 10^6 km.
[j]The cloud's axial magnetic field strength.
[k]The sign of the helicity of the model field lines within the cloud (see text).
[l]The chi-square value, provided by equation (5).
[m]The angle between the axis of the cloud estimated for the last (least squares) iteration and the next to the last.
[n]The symmetry factor defined as $(t_0 \cdot V_f)/(\Delta T \cdot V_c)$, which ideally equals 0.5 when the cloud's center is at the analysis interval center. V_f is typically in the neighborhood of 480 km/s and represents a weighted average of the cloud's speed over the extent from start to time t_0.
[o]The speed of the cloud based on plasma observations (see spacecraft), averaged over interval ΔT.
[p]The speed of the ambient solar wind based on plasma observations averaged over a 10-hour interval upstream of the cloud.
[q]Equal to $V_a - V_c$, which is the solar wind speed across the (upstream) boundary of the cloud.
[r]The spacecraft that provided the magnetometer (MAG) and plasma data used in the analyses, where I1 is IMP 1; I2 is IMP 2; I3 is ISEE 3; I5 is IMP 5; I6 is IMP 6; I7 is IMP 7; I8 is IMP 8; H is HEOS 1; LANL is Los Alamos National Laboratory; and Merge means merged data.

choice. However, from our experience we developed criteria to help choose them according to the results. The associated analysis interval endpoints shown were then considered the "best." As stated above, the criteria depend on (1) the value of χ^2 from the model's fit to the data, (2) the value of δ, and (3) how symmetrical and well centered the magnitude (B) curve of the model is between the endpoints. The cloud in this figure has a reasonably well centered and symmetrical B curve, very small δ (<0.05°), and a small χ^2 (0.43). Hence this is a very well determined case. Notice that θ has a slow "ramp" increase from negative values to positive ones across its extent. This is typical of clouds that have axes that lie in (or near) the ecliptic plane; notice that $\theta_0 = 10°$ in this case. Also $\phi_0 = 105°$, which is typical of clouds at 1 AU, as we will see in the statistical section below. Since $|Y_0|/R_0 = 0.07$, the spacecraft passed very close to the cloud's axis. The duration of the cloud, estimated to be 26 hours, is also typical at 1 AU. The helicity $H = -1$ is apparently a matter of chance; plus and minus are equally likely, according to the statistical results below.

Notice that the model fits the observed θ and ϕ very well and fits only qualitatively well for B, for most of the cloud; the slight deviation at the end for ϕ is exaggerated due to plot folding. We believe that the discrepancy between B^O and B^M at the front of the cloud is probably due to the cloud's interaction with the ambient solar wind, since the cloud has an average speed V_c of 504 km/s, whereas the ambient speed, V_a (the 10-hour average upstream solar wind speed), was 480 km/s, which is only slightly slower, however. This difference could result in a compressed field at the cloud's front and increase B there but not cause much deviation in field direction, which is what we observe. (We will see, however, that this case is somewhat exceptional in this regard in that typically the average upstream speed is faster than the cloud's average speed!) Based on comparison of the curves just before the start time one may think that we could have chosen an earlier start time, but this was attempted and it led to an unacceptable asymmetry in the B model curve.

Figure 3 shows another magnetic cloud, occurring on days 321 and 322 of 1975, in the same format as that of Figure 2. Here, however, the cloud's axis makes a large angle with respect to the ecliptic plane ($\theta_0 = -80°$). As a result the profiles of θ and ϕ are very different from those in Figure 2. For example, θ has a minimum near the middle, and ϕ covers

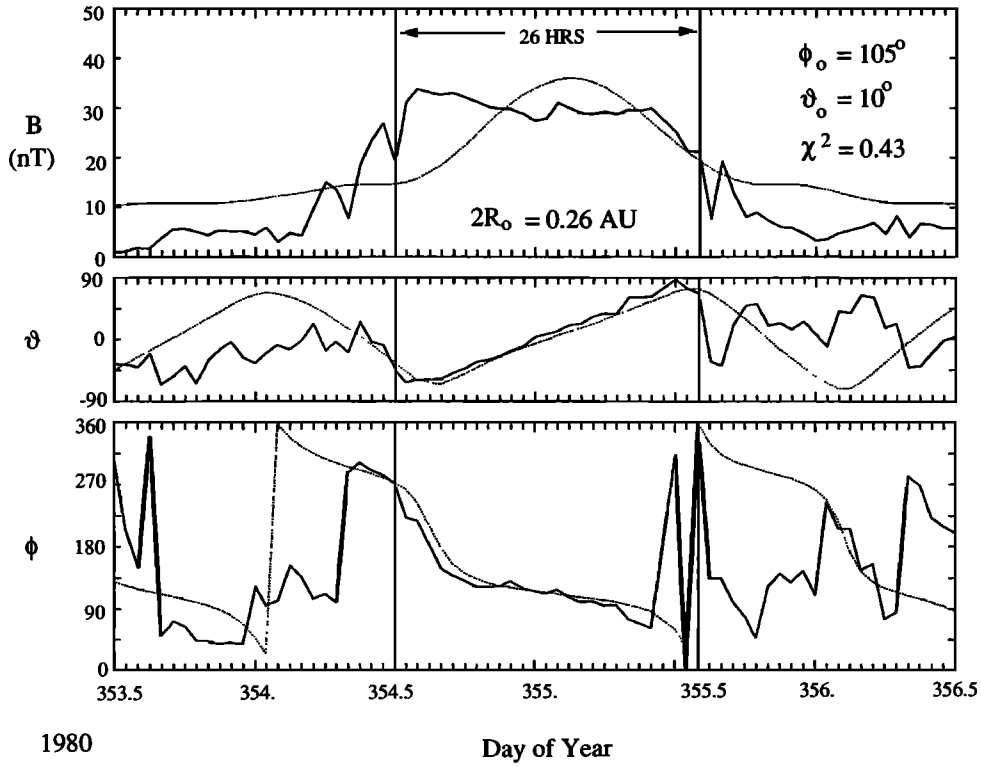

Fig. 2. Three days of magnetic field data (1-hour averages): B is the magnitude, θ is the latitude, and ϕ is the longitude of the field in solar ecliptic coordinates. The solid curves are actual observations from the IMP 8 and ISEE 3 spacecraft. The dotted curves are the resulting model field based on the data in the analysis interval: 1980 day 354, 12 UT, to day 355, 13 UT; these end times are shown by vertical lines. The angles $\phi_0 = 105°$ and $\theta_0 = 10°$ refer to the model's estimate of the attitude of the cloud's axis, and $2R_0 = 0.26$ AU is the estimate of the cloud's diameter. Notice that $Y_0 = 0.07R_0$, which means the spacecraft passed close to the cloud's axis, and the field had negative helicity ($H = -1$).

quite different quadrants. The size is very similar, and B^M is very well centered and symmetrical as in the first case. However, now B^M is above, but close to, B^O near the front of the cloud. This case is consistent with the idea that the cloud–solar wind interaction may result in a slight field rarefaction within the cloud's front region, if the average speed of the cloud ($V_c = 367$ km/s) is slower than the local upstream solar wind (400 km/s), which it was in this case. The spacecraft passed 73% of the way out from the cloud's axis at closest approach, and the duration was 27 hours, about the same as in the first case. Again, helicity is negative, but χ^2 is moderately large (2.02), which is apparently due to the ϕ discrepancy in the center, although plot folding slightly exaggerates its importance in the figure.

Figure 4 shows a third magnetic cloud in the same format and of about the same duration and estimated diameter ($2R_0 = 0.28$ AU) as the other two. It occurs on days 261 and 262 of 1979. Now, however, the axis is tilted out of the ecliptic by $\theta_0 = 78°$. As a result the θ curve has a maximum in the center. As in the first case, B^O is larger than B^M at the front end of the cloud (and B^M is very well centered), but the average speed difference across the front boundary does not explain the field compression. The cloud's average speed, V_c, was 366 km/s, and the ambient solar wind's speed, V_a, was 400 km/s. As we said, this is rather typical of clouds at 1 AU according to our statistics. The model provides a moderately good fit as indicated by a moderate value of $\chi^2 = 1.17$. The spacecraft at closest approach was about halfway out from the axis ($Y_0 = 0.47R_0$), and the helicity was again negative. The discrepancy in ϕ in the middle is again exaggerated by plot folding.

In all three cases the average magnitude of B is above the background, especially if a long-term average of B is considered for background; usually $\langle B \rangle$ is 5.5 nT at 1 AU, if a very long average is taken. For clouds at 1 AU, $\langle B \rangle$ is about 20 nT, almost 4 times background.

Statistical Properties

In this section we determine from our data set some typical attributes of magnetic clouds at 1 AU, near the ecliptic plane. First, the inclination of the axes of the selected magnetic clouds is summarized in Figure 5, which shows the ϕ_0 and $|\theta_0|$ distributions of the axes of the 18 clouds given in Table 1. As we see, $|\theta_0|$ is spread somewhat uniformly over 90° with an average of 42° ± 26°, given at the bottom (in the format of average ± 1 rms). A straight average of θ_0 shows that an average cloud axis at 1 AU is close to the ecliptic plane: $\langle \theta_0 \rangle = -15° \pm 47°$. The distribution of ϕ_0 is given on the left side of the figure where the four dashed lines denote cases where $|\theta_0|$ are very high, as indicated at the top of the $|\theta_0|$ distribution. Obviously in those cases the associated value of ϕ_0 should have less weight in the ϕ_0 distribution. Because of that we show two averages of ϕ_0, one giving the full set and the other, $\langle \phi_0(14) \rangle = 102° \pm 34°$, developed from the 14 values of ϕ_0 that exclude the dashed line cases;

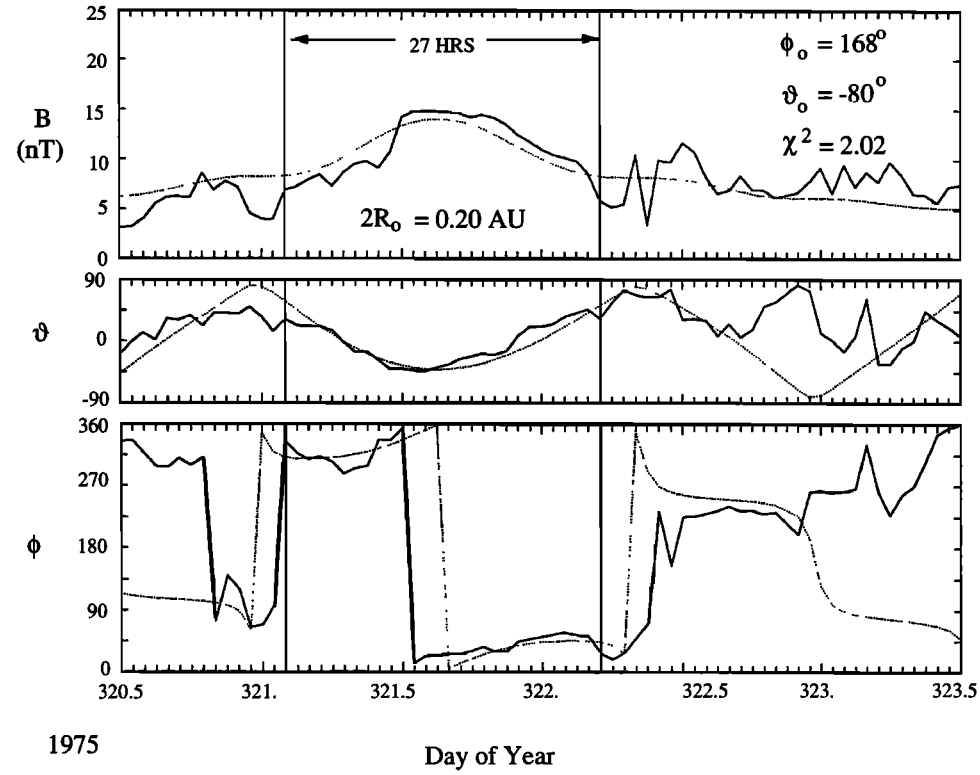

Fig. 3. Three days of magnetic field data in the same format as in Figure 2 where the analysis interval is now 1975, day 321, hour 2, to day 322, hour 5. This cloud is about the same size as that in Figure 2 where $2R_0 = 0.20$ AU, but its axis is tilted steeply: $\phi_0 = 168°$, $\theta_0 = -80°$. Notice that $Y_0 = 0.073\ R_0$ and $H = -1$. The data are from IMP 8.

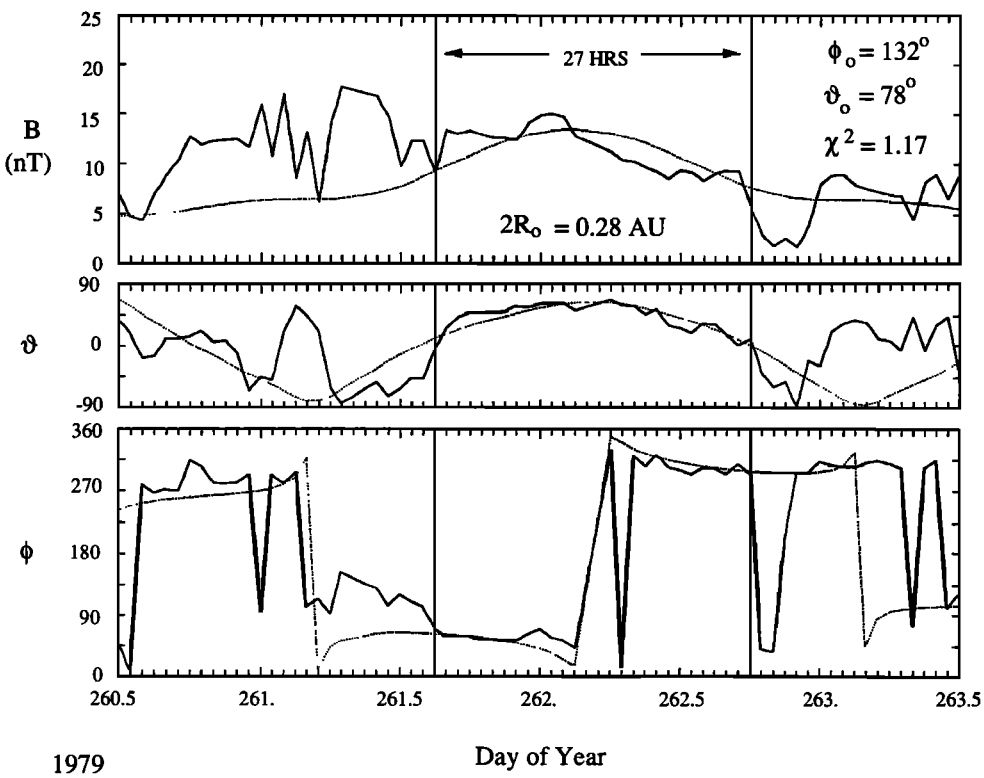

Fig. 4. Three days of magnetic field data in the same format as in Figure 2 where the analysis interval is now 1979, day 261, hour 15, to day 262, hour 18. This cloud is also about the same size as the other two where $2R_0 = 0.28$ AU, but its axis is tilted steeply "upward": $\phi_0 = 132°$ and $\theta_0 = 78°$. Notice that $Y_0 = 0.47R_0$ and $H = -1$. The data are from ISEE 3.

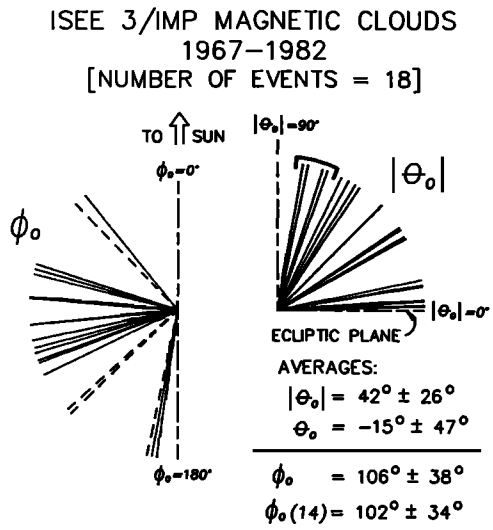

Fig. 5. Distribution of the directions of the estimated axes of the 18 clouds studied in terms of ϕ_0, θ_0, and $|\theta_0|$. The distribution on the left gives ϕ_0 (longitude in the ecliptic plane); $\phi_0 = 0°$ is toward the Sun. On the right is the distribution of $|\theta_0|$ (latitude) measured from the ecliptic plane. The four steep values of $|\theta_0|$ appear as dashed lines in the ϕ_0 distribution. The average ϕ_0 (14) refers to that taken over the 14 solid lines in the ϕ_0 distribution.

the latter is probably the more meaningful average. We see that, on average, the magnetic cloud axes tend to be aligned along the east-west line, within ≈12°.

We calculate the following averages of properties listed in Table 1:

$$2R_0 = 0.28 \text{ AU} \pm 0.095 \text{ AU}$$

$$|Y_0|/R_0 = 0.22 \pm 0.22$$

$$V_c = 446 \text{ km/s} \pm 70 \text{ km/s}$$

$$V_a = 478 \text{ km/s} \pm 90 \text{ km/s}$$

$$B_0 = 19.6 \text{ nT} \pm 6.5 \text{ nT}$$

$$\Delta t = 25.3 \text{ hours} \pm 6.7 \text{ hours}$$

where in each case the uncertainty is ±1 rms. The typical diameter $2R_0$ is a significant fraction of an AU at 1 AU, and the clouds passed the various spacecraft with a big spread of $|Y_0|/R_0$ values, as might be expected, the largest being 0.73, which was uncommon. Large values of $|Y_0|/R_0$ are not likely, because clouds having such values would be difficult to identify. Helicity was almost evenly distributed between positive and negative: 8 were positive and 10 were negative. It is interesting that the product of the average ⟨V⟩ (450 km/s) and the average ⟨Δt⟩ (25.3 hours) is 0.27 AU, which agrees very well with the average of $2R_0$, which is 0.28 AU. This is not too surprising and results, at least in part, from the fact that $V\Delta t$ is a reasonably good estimate of the diameter of a cloud, since the spacecraft usually penetrated a cloud deeply; otherwise the cloud would not have been identified. However, it is somewhat surprising that on average V_a is larger than V_c (by 30 km/s) and in most individual cases V_a is larger than V_c. This is worthy of speculation, but we do not now have a firm explanation.

TABLE 2. Summary of Results of the Statistical Analyses

Parameter	Value
θ_0	−15° ± 47°
$2R_0$	0.28 AU ± 0.095 AU
V_c	446 km/s ± 70 km/s
B_0	19.6 nT ± 6.5 nT
ϕ_0 (14)	102° ± 34°
Y_0/R_0	0.22 ± 0.22
V_a	478 km/s ± 90 km/s
H	8 positive values
	10 negative values

SUMMARY AND DISCUSSION

We have formulated a scheme for optimally fitting the magnetic field in a magnetic cloud to the Lundquist solution, which is based on the assumption of a (locally) cylindrically symmetric force-free field configuration of constant α, and therefore (in cylindrical coordinates)

Axial component

$$B_A = B_0 J_0(\alpha R)$$

Tangential component

$$B_T = B_0 H J_1(\alpha R)$$

Radial component

$$B_R = 0$$

These equations were then used in the following fitting procedure: (1) unit normalization of all magnetic field vectors, (2) variance analysis (provides intermediate eigenvector as an estimate of the direction of the cloud's axis), (3) least squares fit of normalized field data to the above equations, refining the estimate of the cloud's axis, and (4) least squares fit to the "amplitude" B_0.

The seven-parameter fit provides θ_0, ϕ_0 (of cloud's axis),

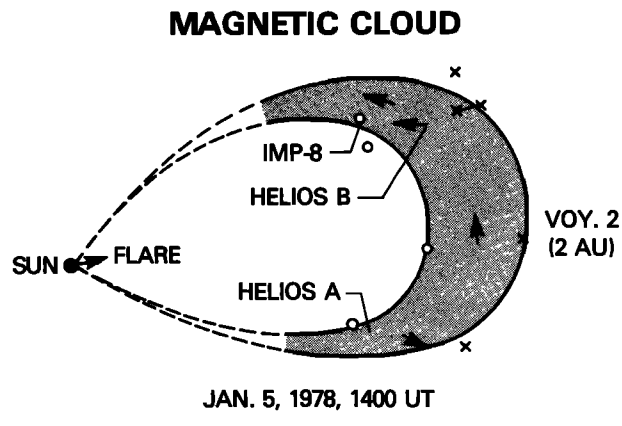

Fig. 6. A sketch of the global configuration of a magnetic cloud [*Burlaga et al.*, 1990] whose characteristics were estimated using the scheme described here where the data was taken from four broadly spaced spacecraft: Helios A and B, IMP 8, and Voyager 2 (located off to the right at 2 AU). The crosses and open circles represent estimated positions for the start and end times of the cloud, respectively, at the various observation points, and the arrows represent the estimated directions of the cloud's axis at the related center points as projected into the ecliptic plane, all for the time 1400 UT of January 5, 1978, as shown.

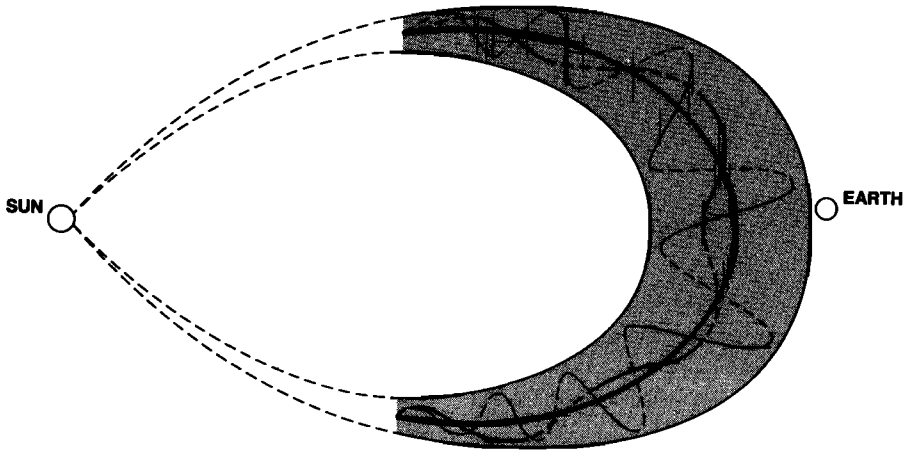

Fig. 7. Based on the *Lundquist* [1950] solution and the results shown in Figure 6, we present here a highly idealized view of the proposed magnetic field line geometry of a "typical" magnetic cloud on a global scale. The thickness of the curves represents field strength, the thicker ones being stronger, and the dashed portions indicate those fields below the ecliptic plane.

closest-approach distance Y_0, amplitude B_0, size α^{-1} (αR_0), helicity $H = \pm 1$, and center time t_0.

The quality of results is based on assessments of χ^2, the symmetry of B(model) according to the value of the so-called symmetry factor, SF (see footnote n of Table 1 for a definition of SF; this is a measure of how far the peak in B(model) is from the center of the analysis interval; ideally they should coincide with SF = 0.5), and the size of δ.

The statistical results of 18 cases at 1 AU (average ± 1 rms) are given in Table 2, based on the individual events listed in Table 1.

The scheme resulted from tests performed with simulated data generated from the model plus "noise" representing realistic data. It was then applied to 23 candidate magnetic clouds, but only 18 survived after scrutiny, which consisted of the application of the scheme and testing of results. Unacceptability depended on large χ^2 or a poorly centered B(model) within the analysis interval, or a lack of convergence (i.e., large δ). Often a few trials, using different analysis intervals for any given case, were necessary, and for a given trial more than one iteration to obtain acceptable values of δ was usually necessary. We point out that according to our quality criteria, results for cases 2 and 8 in Table 1 are probably the most poorly determined of all cases. That is, for case 2, $\chi^2 = 1.26$ (medium value), $\delta = 14.2°$ (big!), and SF = 0.70 (big), and for case 8, $\chi^2 = 4.55$ (big), $\delta = 11.1°$ (big), and SF = 0.62 (medium). On the other hand, cases 1, 3, 10, 12, and 14 are apparently very well determined according to these criteria. All other cases appear to be relatively well determined.

The techniques described here were also employed in order to determine the global configuration of a magnetic cloud observed by spacecraft spread over 2 AU: IMP 8, Helios A and B, and Voyager 2, all sampling portions of a single broadly extended magnetic cloud on January 5, 1978 [*Burlaga et al.*, 1990]. A sketch showing the positions of these spacecraft and the presumed inner and outer boundary positions of the cloud, in ecliptic plane view, is given in Figure 6. How the cloud connects to the solar source is unknown, and therefore in the region close to the Sun it is shown with dashed curves. We consider these results to be a successful application of the scheme described here. If Figure 6 is a faithful indication of the cloud's actual geometry in the ecliptic plane over $\simeq$2 AU and if the field is a force-free configuration of constant α, then the field lines internal to the cloud have a topology similar to that shown in Figure 7, although some distortion may result from the cloud's interaction with the ambient solar wind. Generally then we may consider the field within a magnetic cloud to be represented by that given by Figure 7 or a simple modification of it. An example of simple modification would be the case where the locally observed axis of the cloud is tilted out of the ecliptic plane, requiring a rotation of the overall field configuration shown in Figure 7 about the large-scale symmetry axis aligned with the direction radial to the Sun (approximately the Sun-Earth line in this case).

Early in our introduction we provided the empirical characteristics of a magnetic cloud. Because of our relative success in fitting to a large number of clouds the solutions given by equations (4), which have the property of being cylindrically symmetric, we may add to those characteristics the property of approximate local cylindrical symmetry, at least for clouds at 1 AU.

We believe that the scheme outlined here provides a means of obtaining optimum magnetic cloud parameters consistent with the Lundquist solution. The 18 cases studied provide us with accurate statistics on the local properties of clouds at 1 AU. Their diameters are $\simeq$0.28 AU on average. The peak fields are typically 20 nT, and the average solar wind speed within a cloud is 450 km/s, which is usually (and surprisingly) slower than the ambient solar wind by about 30 km/s. They last for about 25 hours, although for any given case the duration will obviously depend on the closest-approach distance $|Y_0|$, the cloud's orientation, and its speed. As our simulations have shown, the scheme may be useful for helping to determine if a magnetic field and plasma signature in the solar wind is a magnetic cloud, provided reasonable analysis intervals are chosen.

Acknowledgments. We wish to thank Stephanie Myers and Amy Burlaga for helping us with some of the artwork. We thank Bill Mish

for patiently teaching us a few new word processing skills. We are grateful for the usual cooperation that we receive from the National Space Science Data Center, Goddard Space Flight Center, in this case for the supplementary magnetic field and plasma data used in this study.

The Editor thanks M. Berger and W. Gonzalez for their assistance in evaluating this paper.

REFERENCES

Badruddin, R., S. Yadov, N. R. Yadov, and S. P. Agarawal, Influence of magnetic clouds on cosmic ray intensity variations, *Proc. Int. Cosmic Ray Conf. 19th*, *5*, 258, 1985.

Burlaga, L. F., Magnetic clouds: Constant alpha force-free configurations, *J. Geophys. Res.*, *93*, 7217, 1988.

Burlaga, L. F., Magnetic clouds, in *Physics of the Inner Heliosphere*, edited by L. Lanzerotti, R. Schwenn, and E. Marsch, chap. 6, Springer-Verlag, New York, in press, 1989.

Burlaga, L. F., and K. W. Behannon, Magnetic clouds: Voyager observations between 2 and 4 AU, *Sol. Phys.*, *81*, 181, 1982.

Burlaga, L. F., E. Sittler, F. Mariani, and R. Schwenn, Magnetic loop behind an interplanetary shock: Voyager, Helios, and IMP 8 observations, *J. Geophys. Res.*, *86*, 6673, 1981.

Burlaga, L. F., K. W. Behannon, and L. W. Klein, Compound streams, magnetic clouds, and major geomagnetic storms, *J. Geophys. Res.*, *92*, 5725, 1987.

Burlaga, L. F., R. Lepping, and J. Jones, Global configuration of a magnetic cloud, in *Physics of Magnetic Flux Ropes*, *Geophys. Monogr. Ser.*, vol. 58, edited by C. T. Russell, E. R. Priest, and L. C. Lee, p. 373, AGU, Washington, D. C., 1990.

Elphic, R. C., and C. T. Russell, Magnetic flux ropes in the Venus ionosphere: Observations and models, *J. Geophys. Res.*, *88*, 58, 1983.

Goldstein, H., On the field configuration in magnetic clouds, Solar Wind Five, *NASA Conf. Publ.*, *2280*, 731, 1983.

Ipavich, F. M. and R. P. Lepping, Analysis of the October 31, 1972 interplanetary shock wave and associated unusual phenomena, *Proc. Int. Cosmic Ray Conf. 14th*, *5*, 1829, 1975.

Ivanov, K. G., A. F. Harshiladze, E. G. Eroshenko, and V. A. Styazhkin, Configuration, structure and dynamics of magnetic clouds from solar flares in light of measurements on board VEGA 1 and VEGA 2 in January–February, 1986, *Sol. Phys.*, *120*, 407, 1989.

Klein, L. W., and L. F. Burlaga, Interplanetary magnetic clouds at 1 AU, *J. Geophys. Res.*, *87*, 613, 1982.

Lundquist, S., Magnetohydrostatic fields, *Ark. Fys.*, *2*, 361, 1950.

Marubashi, K., Structure of the interplanetary magnetic clouds and their solar origins, *Adv. Space Res.*, *6*(6), 335, 1986.

Morrison, P., Solar-connected variations of the cosmic rays, *Phys. Rev.*, *95*, 646, 1954.

Sonnerup, B. U. O., and L. J. Cahill, Magnetopause structure and attitude from Explorer 12 observations, *J. Geophys. Res.*, *72*, 171, 1967.

Suess, S. T., Magnetic clouds and the pinch effect, *J. Geophys. Res.*, *93*, 5437, 1988.

Taylor, J. B. Relaxation and magnetic reconnection in plasmas, *Rev. Mod. Phys. 58*(3), 741, 1986.

Whang, Y. C., Forward-reverse shock pairs associated with coronal mass ejections, *J. Geophys. Res.*, *93*, 5897, 1988.

Wilson, R. M., Geomagnetic response to magnetic clouds, *Planet. Space Sci.*, *35*, 329, 1987.

Wilson, R. M., and E. Hildner, Are interplanetary magnetic clouds manifestations of coronal transients at 1 AU?, *Sol. Phys.*, *91*, 169, 1984.

Wilson, R. M., and E. Hildner, On the association of magnetic clouds with disappearing filaments, *J. Geophys. Res.*, *91*, 5867, 1986.

Woltjer, L., A theorem on force-free magnetic fields, *Proc. Nat. Acad. Sci. U.S.A.*, *44*(6), 389, 1958.

Yang, W.-H., Expansion of solar-terrestrial low-β plasmoid, *Astrophys. J.*, *344*, 966, 1989.

Zhang, G., and L. F. Burlaga, Magnetic clouds, geomagnetic disturbances, and cosmic ray decreases, *J. Geophys. Res.*, *93*, 2511, 1988.

L. F. Burlaga and R. P. Lepping, Laboratory for Extraterrestrial Physics, NASA Goddard Space Flight Center, Greenbelt, MD 20771.

J. A. Jones, STX, 4400 Forbes Boulevard, Lanham, MD 20706.

(Received September 13, 1989;
revised December 11, 1989;
accepted January 15, 1990.)